FAIR NORMALIZING FLOWS

Anonymous authors
Paper under double-blind review

ABSTRACT

Fair representation learning is an attractive approach that promises fairness of downstream predictors by encoding sensitive data. Unfortunately, recent work has shown that strong adversarial predictors can still exhibit unfairness by recovering sensitive attributes from these representations. In this work, we present Fair Normalizing Flows (FNF), a new approach offering more rigorous fairness guarantees for learned representations. Specifically, we consider a practical setting where we can estimate the probability density for sensitive groups. The key idea is to model the encoder as a normalizing flow trained to minimize the statistical distance between the latent representations of different groups. The main advantage of FNF is that its exact likelihood computation allows us to obtain guarantees on the maximum unfairness of any potentially adversarial downstream predictor. We experimentally demonstrate the effectiveness of FNF in enforcing various group fairness notions, as well as other attractive properties such as interpretability and transfer learning, on a variety of challenging real-world datasets.

1 INTRODUCTION

As machine learning is being increasingly used in scenarios that can negatively affect humans (Brennan et al., 2009; Khandani et al., 2010; Barocas & Selbst, 2016), fair representation learning has become one of the most promising ways to encode data into new, unbiased representations with high utility. Concretely, the goal is to ensure that representations have two properties: (i) they are informative for various prediction tasks of interest, (ii) sensitive attributes of the original data (e.g., race) cannot be recovered from the representations. Perhaps the most prominent approach for learning fair representations is adversarial training (Edwards & Storkey, 2016; Madras et al., 2018; Xie et al., 2017; Song et al., 2019; Roy & Boddeti, 2019) which jointly trains an encoder trying to transform data into a fair representation with an adversary attempting to recover sensitive attributes from the representation. However, several recent lines of work (Feng et al., 2019; Moyer et al., 2018; Elazar & Goldberg, 2018; Xu et al., 2020; Gupta et al., 2021; Song & Shmatikov, 2020) have noticed that these approaches do not produce truly fair representations: stronger adversaries *can* in fact recover sensitive attributes. Clearly, this could allow malicious or ignorant users to use the provided representations to discriminate. This problem emerges at a time when regulators are crafting rules (Whittaker et al., 2018; EU, 2021; FTC, 2021) on the fair usage of AI, stating that any entity that cannot guarantee non-discrimination would be held accountable for the produced data. This raises the question: *Can we learn representations which provably guarantee that sensitive attributes cannot be recovered?*

This work Following prior work, we focus on tabular datasets used for tasks such as loan or insurance asessment where fairness is of high relevance. We assume that the original input data $\boldsymbol{x}$ comes from two probability distributions p_0 and p_1, representing groups with sensitive attributes $a = 0$ and $a = 1$, respectively. In the cases where distributions p_0 and p_1 are known, we will obtain provable fairness guarantees, and otherwise we perform density estimation and obtain guarantees with respect to the estimated distribution. In our experimental evaluation we confirm that the bounds computed on the estimated distribution in practice also bound adversarial accuracy on the true distribution, meaning that density estimation works well for the setting we consider.

To address the above challenges, we propose Fair Normalizing Flows (FNF), a new method for learning fair representations with guarantees. In contrast to other approaches where encoders are standard feed-forward neural networks, we instead model the encoder as a normalizing flow (Rezende & Mohamed, 2015). Fig. 1 provides a high-level overview of FNF. As shown on the left in Fig. 1,

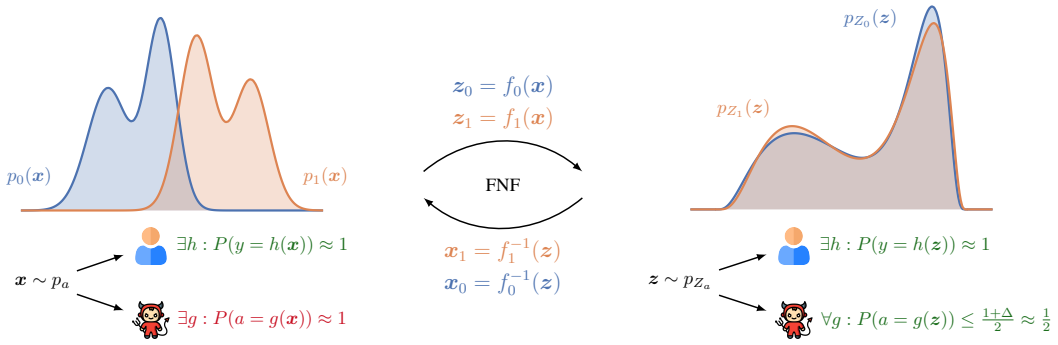

Figure 1: Overview of Fair Normalizing Flows (FNF). There are two encoders, f_0 and f_1, that transform the two input distributions p_0 and p_1 into latent distributions p_{Z_0} and p_{Z_1} with a small statistical distance $\Delta \approx 0$. Without FNF, a strong adversary g can easily recover sensitive attribute a from the original input $\boldsymbol{x}$, but once inputs are passed through FNF, we are guaranteed that *any* adversary that tries to guess sensitive attributes from latent $\boldsymbol{z}$ can not be significantly better than random chance. At the same time, we can ensure that any benevolent user h maintains high utility.

using raw inputs $\boldsymbol{x}$ allows us to train high-utility classifiers h, but at the same time does not protect against the existence of a malicious adversary g that can predict a sensitive attribute a from the features in $\boldsymbol{x}$. Our architecture consists of two flow-based encoders f_0 and f_1, where flow f_a transforms probability distribution $p_a(\boldsymbol{x})$ into $p_{Z_a}(\boldsymbol{z})$ by mapping $\boldsymbol{x}$ into $\boldsymbol{z} = f_a(\boldsymbol{x})$. The goal of the training procedure is to minimize the distance Δ between the resulting distributions $p_{Z_0}(\boldsymbol{z})$ and $p_{Z_1}(\boldsymbol{z})$ so that an adversary cannot distinguish between them. Intuitively, after training our encoder, each latent representation $\boldsymbol{z}$ can be inverted into original inputs $x_0 = f_0^{-1}(\boldsymbol{z})$ and $x_1 = f_1^{-1}(\boldsymbol{z})$ that should ideally have similar probability w.r.t. p_0 and p_1, meaning that even the optimal adversary cannot distinguish which of them actually produced latent $\boldsymbol{z}$. Crucially, as normalizing flows enable us to compute the exact likelihood in the latent space, for trained encoders we can upper bound the accuracy of *any* adversary with $\frac{1+\Delta}{2}$, which should be small if training was successful. Furthermore, the distance Δ provides a tight upper bound (Madras et al., 2018) on common fairness notions such as demographic parity (Dwork et al., 2012) and equalized odds (Hardt et al., 2016). As shown on the right in Fig. 1, we can still train high-utility classifiers h using our representations, but now we can actually *guarantee* that no adversary g can recover sensitive attributes better than chance.

We empirically demonstrate that FNF can substantially increase provable fairness without significantly sacrificing accuracy on several common datasets. Additionally, we show that the invertibility of FNF enables algorithmic recourse, allowing us to examine how to reverse a negative decision outcome.

Main contributions Our key contributions are:

- A novel fair representation learning method, called Fair Normalizing Flows (FNF), which can guarantee that sensitive attributes cannot be recovered from the learned representations.
- Experimental evaluation demonstrating that FNF can provably remove sensitive attributes from the representations, while keeping accuracy for the prediction task sufficiently high.
- Extensive investigation of algorithmic recourse and applications of FNF to transfer learning.

2 Related Work

In this work, we focus on group fairness, which requires certain classification statistics to be equal across different groups of the population. Concretely, we consider demographic parity (Dwork et al., 2012), equalized odds (Hardt et al., 2016), and equality of opportunity (Hardt et al., 2016), which are widely studied in the literature (Edwards & Storkey, 2016; Madras et al., 2018; Zemel et al., 2013). Algorithms enforcing such fairness notions target various stages of the machine learning pipeline: Pre-processing methods transform sensitive data into an unbiased representation (Zemel et al., 2013; McNamara et al., 2019), in-processing methods modify training by incorporating fairness

constraints (Kamishima et al., 2011; Zafar et al., 2017), and post-processing methods change the predictions of a pre-trained classifier (Hardt et al., 2016). Here, we consider fair representation learning (Zemel et al., 2013), which computes data representations that hide sensitive information, e.g. group membership, while maintaining utility for downstream tasks and allowing transfer learning.

Fair representation learning Fair representations can be learned with a variety of different approaches, including variational autoencoders (Moyer et al., 2018; Louizos et al., 2016), adversarial training (Edwards & Storkey, 2016; Madras et al., 2018; Xie et al., 2017; Song et al., 2019; Roy & Boddeti, 2019; Liao et al., 2019; Jaiswal et al., 2020; Feng et al., 2019), and disentanglement (Creager et al., 2019; Locatello et al., 2019). Adversarial training methods minimize a lower bound on demographic parity, namely an adversary's accuracy for predicting the sensitive attributes from the latent representation. However, since these methods only empirically evaluate worst-case unfairness, adversaries that are not considered during training can still recover sensitive attributes from the learned representations (Feng et al., 2019; Moyer et al., 2018; Elazar & Goldberg, 2018; Xu et al., 2020; Gupta et al., 2021; Song & Shmatikov, 2020). These findings illustrate the necessity of learning representations with provable guarantees on the maximum recovery of sensitive information regardless of the adversary, which is precisely the goal of our work. Prior work makes first steps in this direction: Gupta et al. (2021) upper bound a monotonically increasing function of demographic parity with the mutual information between the latent representation and sensitive attributes. However, the monotonic nature of this bound precludes computing guarantees on the reconstruction power of the optimal adversary. Feng et al. (2019) minimize the Wasserstein distance between latent distributions of different protected groups, but only provide an upper bound on the performance of any Lipschitz continuous adversary. However, as we will show, the optimal adversary is generally discontinuous.

Provable fairness guarantees The ongoing development of guidelines on the fair usage of AI (Whittaker et al., 2018; EU, 2021; FTC, 2021) has spurred interest in provably fair algorithms. Unlike this work, the majority of these efforts (McNamara et al., 2019; John et al., 2020; Urban et al., 2020; Ruoss et al., 2020) focus on individual fairness. Individual fairness is also tightly linked to differential privacy (Dwork et al., 2012; 2006), which guarantees that an attacker cannot infer whether a given individual was present in the dataset or not, but these models can still admit reconstruction of sensitive attributes by leveraging population-level correlations (Jagielski et al., 2019). Group fairness certification methods (Albarghouthi et al., 2017; Bastani et al., 2019; Segal et al., 2020) generally only focus on certification and, unlike our work, do not learn representations that are provably fair.

3 BACKGROUND

We assume that the data $(\boldsymbol{x}, a) \in \mathbb{R}^d \times \mathcal{A}$ comes from a probability distribution p, where $\boldsymbol{x}$ represents the features and a represents a sensitive attribute. In this work, we focus on the case where the sensitive attribute is binary, meaning $\mathcal{A} = \{0, 1\}$. Given p, we can define the conditional probabilities as $p_0(\boldsymbol{x}) = P(\boldsymbol{x}|a = 0)$ and $p_1(\boldsymbol{x}) = P(\boldsymbol{x}|a = 1)$. We are interested in classifying each sample $(\boldsymbol{x}, a)$ to a label $y \in \{0, 1\}$, which may or may not be correlated with the sensitive attribute a. Our goal is to build a classifier $\hat{y} = h(\boldsymbol{x})$ which tries to predict y from the features $\boldsymbol{x}$, while satisfying certain notions of fairness. Next, we present several definitions of fairness relevant for this work.

Fairness criteria A classifier h satisfies *demographic parity* if it assigns positive outcomes to both sensitive groups equally likely, i.e., $P(h(\boldsymbol{x}) = 1|a = 0) = P(h(\boldsymbol{x}) = 1|a = 1)$. In cases where demographic parity can not be satisfied, we are also interested in a metric called demographic parity distance, defined as $|\mathbb{E}[h(\boldsymbol{x})|a = 0] - \mathbb{E}[h(\boldsymbol{x})|a = 1]|$. A possible issue with demographic parity occurs if the base rates differ among the attributes, i.e., $P(y = 1|a = 0) \neq P(y = 1|a = 1)$. In that case, even the ground truth label y does not satisfy demographic parity. To address this, Hardt et al. (2016) instead introduced *equalized odds*, which requires that $P(h(\boldsymbol{x}) = 1|y = y_0, a = 0) = P(h(\boldsymbol{x}) = 1|y = y_0, a = 1)$ for $y_0 \in \{0, 1\}$, assuming $h(\boldsymbol{x}) = 1$ is the advantaged outcome.

Fair representations Instead of directly predicting y from $\boldsymbol{x}$, Zemel et al. (2013) introduced the idea of learning *fair representations* of data. The idea is that a data producer can preprocess the original data $\boldsymbol{x}$ and obtain a new representation $\boldsymbol{z} = f(\boldsymbol{x}, a)$. Then, any data consumer, who is using this data to solve a downstream task, can use $\boldsymbol{z}$ as an input to the classifier instead of the original data

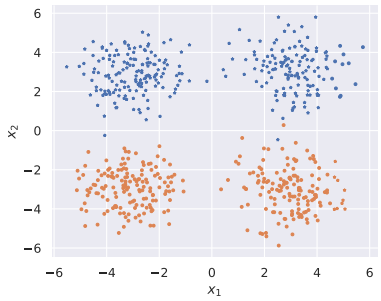

Figure 2: Samples from our example distribution. The blue group ($a = 0$) is sampled from p_0 and the orange group ($a = 1$) is sampled from p_1.

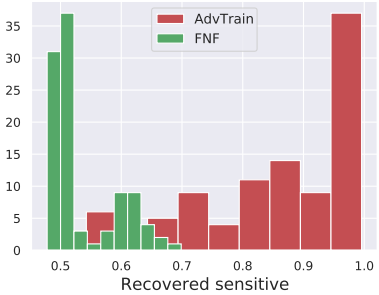

Figure 3: Sensitive attribute recovery rates for adversarial training and fair normalizing flows (FNF) with 100 different random seeds.

$\boldsymbol{x}$. Thus, if the data producer can ensure that data representation is fair (w.r.t. some notion of fairness), then all classifiers built on top of this representation will automatically inherit the fairness property.

Normalizing flows Flow-based generative models (Rezende & Mohamed, 2015; Dinh et al., 2015; 2016; Kingma & Dhariwal, 2018) provide an attractive framework for transforming any probability distribution q into another distribution $\bar{q}$. Accordingly, they are often used to estimate densities from data using the *change of variables* formula on a sequence of invertible transformations, so-called normalizing flows (Rezende & Mohamed, 2015). In this work, however, we mainly leverage the fact that flow models sample a latent variable $\boldsymbol{z}$ from a density $\bar{q}(\boldsymbol{z})$ and apply an invertible function $f_{\boldsymbol{\theta}}$, parametrized by $\boldsymbol{\theta}$, to obtain datapoint $\boldsymbol{x} = f_{\boldsymbol{\theta}}^{-1}(\boldsymbol{z})$. Given a density $q(\boldsymbol{x})$, the exact log-likelihood is then obtained by applying the change of variables formula $\log q(\boldsymbol{x}) = \log \bar{q}(\boldsymbol{z}) + \log |\det(d\boldsymbol{z}/d\boldsymbol{x})|$. Thus, for $f_{\boldsymbol{\theta}} = f_1 \circ f_2 \circ \ldots \circ f_K$ with $\boldsymbol{r}_0 = \boldsymbol{x}$, $f_i(\boldsymbol{r}_{i-1}) = \boldsymbol{r}_i$, and $\boldsymbol{r}_K = \boldsymbol{z}$, we have

$$\log q(\boldsymbol{x}) = \log \bar{q}(\boldsymbol{z}) + \sum_{i=1}^{K} \log |\det(d\boldsymbol{r}_i/d\boldsymbol{r}_{i-1})|. \tag{1}$$

A clever choice of transformations f_i (Rezende & Mohamed, 2015; Dinh et al., 2015; 2016) makes the computation of log-determinant tractable, resulting in efficient training and sampling. Alternative generative models cannot compute the exact log-likelihood (e.g., VAEs (Kingma & Welling, 2014), GANs (Goodfellow et al., 2014)) or have inefficient sampling (e.g., autoregressive models). Our approach is related to the work on alignment flows (Grover et al., 2020; Usman et al., 2020), but the key difference is that they jointly learn the density and the transformation, which is not applicable in the fairness setting where these can be computed by different entities (data regulator and data producer). Discrete flows (Tran et al., 2019; Hoogeboom et al., 2019) are also related to our approach, and can be applied for discrete datasets.

4 Motivation

In this section, we motivate our approach by highlighting some key issues with fair representation learning based on adversarial training. Consider a distribution of samples $\boldsymbol{x} = (x_1, x_2) \in \mathbb{R}^2$ divided into two groups, shown as blue and orange in Fig. 2. The first group with a sensitive attribute $a = 0$ has a distribution $(x_1, x_2) \sim p_0$, where p_0 is a mixture of two Gaussians $\mathcal{N}([-3, 3], I)$ and $\mathcal{N}([3, 3], I)$. The second group with a sensitive attribute $a = 1$ has a distribution $(x_1, x_2) \sim p_1$, where p_1 is a mixture of two Gaussians $\mathcal{N}([-3, -3], I)$ and $\mathcal{N}([3, -3], I)$. The label of a point (x_1, x_2) is defined by $y = 1$ if $\text{sign}(x_1) = \text{sign}(x_2)$ and $y = 0$ otherwise. Our goal is to learn a data representation $\boldsymbol{z} = f(\boldsymbol{x}, a)$ such that it is *impossible* to recover a from $\boldsymbol{z}$, but still possible to predict target y from $\boldsymbol{z}$. Note that such a representation exists for our task: simply setting $\boldsymbol{z} = f(\boldsymbol{x}, a) = (-1)^a \boldsymbol{x}$ makes it impossible to predict whether a particular $\boldsymbol{z}$ corresponds to $a = 0$ or $a = 1$, while still allowing us to train a classifier h with essentially perfect accuracy (e.g., $h(\boldsymbol{z}) = \mathbb{1}_{\{z_1 > 0\}}$).

Adversarial training for fair representations One of the most popular approaches to this problem is adversarial training (Edwards & Storkey, 2016; Madras et al., 2018). The idea is to train encoder

f and classifier h jointly with an adversary g that tries to predict sensitive attribute a. While the adversary tries to minimize its loss $\mathcal{L}_{adv}$, the encoder f and classifier h are trying to maximize $\mathcal{L}_{adv}$ and minimize the classification loss $\mathcal{L}_{clf}$.

$$\min_{f,h} \max_{g \in \mathcal{G}} \mathbb{E}_{(\boldsymbol{x},a)\sim D} \left[\mathcal{L}_{clf}(f(\boldsymbol{x}, a), h) - \gamma \mathcal{L}_{adv}(f(\boldsymbol{x}, a), g) \right], \tag{2}$$

where $\mathcal{G}$ denotes the model family of adversaries, e.g., neural networks, considered during training. Unfortunately, there are two key issues with adversarial training. First, it yields a non-convex optimization problem which usually cannot be solved to optimality because of saddle points (extensively studied for GANs (Berard et al., 2020)). Second, it assumes that the adversary g comes from a fixed model family $\mathcal{G}$, which means that even if the optimal $g \in \mathcal{G}$ cannot recover the sensitive attribute a, adversaries from other model families can still do so as demonstrated in recent work (Feng et al., 2019; Moyer et al., 2018; Elazar & Goldberg, 2018; Xu et al., 2020; Gupta et al., 2021). To investigate these issues, we apply adversarial training to learn representations for our synthetic example, and measure how often the sensitive attributes can be recovered from learned representations. Our results, shown in Fig. 3, repeated 100 times with different seeds, demonstrate that adversarial training is unstable and rarely results in truly fair representations (where only 50% can be recovered). In Section 6 we follow up on recent work and show that several adversarial fair representation learning approaches are not robust to adversaries from a different model familiy (e.g., larger networks). In Fig. 3 we show that our approach, introduced next, can reliably produce fair representations without affecting utility.

5 Fair Normalizing Flows

Throughout this section we will assume knowledge of prior distributions $p_0(\boldsymbol{x})$ and $p_1(\boldsymbol{x})$. At the end of the section, we discuss the required changes if we only work with estimates. Let $\mathcal{Z}_0$ and $\mathcal{Z}_1$ denote conditional distributions of $z = f(\boldsymbol{x}, a)$ for $a \in \{0, 1\}$, and let p_{Z_0} and p_{Z_1} denote their respective densities. Madras et al. (2018) have shown that bounding the *statistical distance* $\Delta(p_{Z_0}, p_{Z_1})$ between $\mathcal{Z}_0$ and $\mathcal{Z}_1$ provides an upper bound on the unfairness of any classifier h built on top of the representation encoded by f. The statistical distance between $\mathcal{Z}_0$ and $\mathcal{Z}_1$ is defined as the maximum mean discrepancy (MMD) (Gretton et al., 2006) between the two distributions:

$$\Delta(p_{Z_0}, p_{Z_1}) \triangleq \sup_{\mu} |\mathbb{E}_{\boldsymbol{z}\sim\mathcal{Z}_0}[\mu(\boldsymbol{z})] - \mathbb{E}_{\boldsymbol{z}\sim\mathcal{Z}_1}[\mu(\boldsymbol{z})]|, \tag{3}$$

where $\mu\colon \mathbb{R}^d \to \{0, 1\}$ is a binary classifier trying to discriminate between $\mathcal{Z}_0$ and $\mathcal{Z}_1$. If we can train an encoder to induce latent distributions $\mathcal{Z}_0$ and $\mathcal{Z}_1$ with statistical distance below some threshold, then we can both upper bound the maximum adversarial accuracy by $(1 + \Delta(p_{Z_0}, p_{Z_1}))/2$ and, using the bounds from Madras et al. (2018), obtain guarantees for demographic parity and equalized odds of any downstream classifier h. Such guarantees are unattainble for adversarial training, which minimizes a lower bound of $\Delta(p_{Z_0}, p_{Z_1})$. In contrast, we learn fair representations that allow computing the optimal adversary μ^* attaining the supremum in Eq. (3) and thus enable exact evaluation of $\Delta(p_{Z_0}, p_{Z_1})$.

Optimal adversary In the following lemma we state the form of an optimal adversary which attains the supremum in the definition of statistical distance in Eq. (3). We show the proof in Appendix A.1.

Lemma 5.1. *The adversary μ^* attaining the supremum in the definition of $\Delta(p_{Z_0}, p_{Z_1})$ can be defined as $\mu^*(\boldsymbol{z}) = \mathbb{1}_{\{p_{Z_0}(\boldsymbol{z}) \leq p_{Z_1}(\boldsymbol{z})\}}$, namely it evaluates to 1 if and only if $p_{Z_0}(\boldsymbol{z}) \leq p_{Z_1}(\boldsymbol{z})$.*

This intuitively makes sense – given some representation $\boldsymbol{z}$, the adversary computes likelihood under both distributions $\mathcal{Z}_0$ and $\mathcal{Z}_1$, and predicts the attribute with higher likelihood for that $\boldsymbol{z}$. Liao et al. (2019) also observed that the optimal adversary can be phrased as $\arg\max_a p(a|\boldsymbol{z})$. So far, prior work mostly focused on mapping input $\boldsymbol{x}$ to the latent representation $\boldsymbol{z} = f_\theta(\boldsymbol{x}, a)$ via standard neural networks. However, for such models, given densities $p_0(\boldsymbol{x})$ and $p_1(\boldsymbol{x})$ over the input space, it is intractable to compute the densities $p_{Z_0}(\boldsymbol{z})$ and $p_{Z_1}(\boldsymbol{z})$ in the latent space as many inputs $\boldsymbol{x}$ can be mapped to the same latent $\boldsymbol{z}$ and we cannot use inverse function theorem. Consequently, prior adversarial training methods cannot compute the optimal adversary and thus resort to a lower bound.

Encoding with normalizing flows Our approach, named Fair Normalizing Flows (FNF), consists of two models, f_0 and f_1, that encode inputs from the groups with sensitive attributes $a = 0$ and

$a = 1$, respectively. We show a high-level overview of FNF in Fig. 1. Note that models f_0 and f_1 are parameterized by θ_0 and θ_1, but we do not write this explicitly to ease the notation. Given some input $\boldsymbol{x}_0 \sim p_0$, it is encoded to $\boldsymbol{z}_0 = f_0(\boldsymbol{x}_0)$, inducing a probability distribution $\mathcal{Z}_0$ with density $p_{Z_0}(\boldsymbol{z})$ over all possible latent representations $\boldsymbol{z}$. Similarly, inputs $\boldsymbol{x}_1 \sim p_1$ are encoded to $\boldsymbol{z}_1 = f_1(\boldsymbol{x}_1)$, inducing the probability distribution $\mathcal{Z}_1$ with density $p_{Z_1}(\boldsymbol{z})$. Clearly, if we can train f_0 and f_1 so that the resulting distributions $\mathcal{Z}_0$ and $\mathcal{Z}_1$ have small distance, then we can guarantee fairness of representations using bounds from Madras et al. (2018). As evaluating statistical distance is intractable for most neural networks, we need a model family that allows us to compute this quantity.

We propose to use bijective encoders f_0 and f_1 based on normalizing flows (Rezende & Mohamed, 2015; Dinh et al., 2016). Normalizing flows allow us to compute the densities at $\boldsymbol{z}$, using the change of variables formula

$$\log p_{Z_a}(\boldsymbol{z}) = \log p_a(f_a^{-1}(\boldsymbol{z})) + \log \left| \det \frac{\partial f_a^{-1}(\boldsymbol{z})}{\partial \boldsymbol{z}} \right| \tag{4}$$

for $a \in \{0, 1\}$. We can thus write the optimal adversary as $\mu^*(\boldsymbol{z}) = \mathbb{1}_{\{p_{Z_0}(\boldsymbol{z}) \leq p_{Z_1}(\boldsymbol{z})\}}$. To compute the statistical distance it remains to evaluate the expectations $\mathbb{E}_{\boldsymbol{z}\sim\mathcal{Z}_0}[\mu^*(\boldsymbol{z})]$ and $\mathbb{E}_{\boldsymbol{z}\sim\mathcal{Z}_1}[\mu^*(\boldsymbol{z})]$. Sampling from $\mathcal{Z}_0$ and $\mathcal{Z}_1$ is straightforward – we can sample $\boldsymbol{x}_0 \sim p_0$ and $\boldsymbol{x}_1 \sim p_1$, and then pass the samples $\boldsymbol{x}_0$ and $\boldsymbol{x}_1$ through the respective encoders f_0 and f_1 to obtain $\boldsymbol{z}_0 \sim \mathcal{Z}_0$ and $\boldsymbol{z}_1 \sim \mathcal{Z}_1$. Given that the outputs of μ^* are bounded between 0 and 1, we can then use Hoeffding inequality to compute the confidence intervals for our estimate using a finite number of samples.

Lemma 5.2. *Given a finite number of samples $\boldsymbol{x}_0^1, \boldsymbol{x}_0^2, ..., \boldsymbol{x}_0^n \sim p_0$ and $\boldsymbol{x}_1^1, \boldsymbol{x}_1^2, ..., \boldsymbol{x}_1^n \sim p_1$, denote as $\boldsymbol{z}_0^i = f_0(\boldsymbol{x}_0^i)$ and $\boldsymbol{z}_1^i = f_1(\boldsymbol{x}_1^i)$ and let $\hat{\Delta}(p_{Z_0}, p_{Z_1}) := |\frac{1}{n}\sum_{i=1}^n \mu^*(\boldsymbol{z}_0^i) - \frac{1}{n}\sum_{i=1}^n \mu^*(\boldsymbol{z}_1^i)|$ be an empirical estimate of the statistical distance $\Delta(p_{Z_0}, p_{Z_1})$. Then, for $n \geq -2\log(1-\sqrt{1-\delta})/\epsilon^2$ with probability at least $1-\delta$, we are guaranteed that $\Delta(p_{Z_0}, p_{Z_1}) \leq \hat{\Delta}(p_{Z_0}, p_{Z_1}) + \epsilon$.*

Lemma 5.3. *We can bound $\Delta(p_{Z_0}, p_{Z_1})^2 \leq \frac{1}{4}(KL(p_{Z_0}, p_{Z_1}) + KL(p_{Z_1}, p_{Z_0}))$.*

Training flow-based encoders The next challenge is to design a training procedure for our newly proposed architecture. The main issue is that the statistical distance is not differentiable (as classifier μ^* is binary) so we replace it with a differentiable proxy based on symmetrized KL divergence, shown in Lemma 5.3 (proof is shown in **??**). We show a high-level description of our training procedure in Algorithm 1. In each step, we sample a batch of $\boldsymbol{x}_0$ and $\boldsymbol{x}_1$ from the respective distributions and encode them to the representations $\boldsymbol{z}_0$ and $\boldsymbol{z}_1$. We then estimate a symmetrized KL divergence between distributions $\mathcal{Z}_0$ and $\mathcal{Z}_1$, denoted as $\mathcal{L}_0 + \mathcal{L}_1$, and combine it with a classification loss $\mathcal{L}_{clf}$ using tradeoff parameter γ, and run a gradient step to minimize the joint loss. While we use a convex scalarization scheme to obtain the joint loss in Algorithm 1, our approach is independent of the concrete multi-objective optimization objective. We will demonstrate the compatibility with other scalarization schemes in Appendix C.

Algorithm 1 Learning Fair Normalizing Flows

Input: N, B, γ, p_0, p_1
Initialize f_0 and f_1 with parameters θ_0 and θ_1
for $i = 1$ **to** N **do**
  for $j = 1$ **to** B **do**
    Sample $\boldsymbol{x}_0^j \sim p_0, \boldsymbol{x}_1^j \sim p_1$
    $\boldsymbol{z}_0^j = f_0(\boldsymbol{x}_0^j)$
    $\boldsymbol{z}_1^j = f_1(\boldsymbol{x}_1^j)$
  end for
  $\mathcal{L}_0 = \frac{1}{B}\sum_{j=1}^B(\log p_{Z_0}(\boldsymbol{z}_0^j) - \log p_{Z_1}(\boldsymbol{z}_0^j))$
  $\mathcal{L}_1 = \frac{1}{B}\sum_{j=1}^B(\log p_{Z_1}(\boldsymbol{z}_1^j) - \log p_{Z_0}(\boldsymbol{z}_1^j))$
  $\mathcal{L} = \gamma(\mathcal{L}_0 + \mathcal{L}_1) + (1-\gamma)\mathcal{L}_{clf}$
  Update $\theta_0 \leftarrow \theta_0 - \alpha\nabla_{\theta_0}\mathcal{L}$
  Update $\theta_1 \leftarrow \theta_1 - \alpha\nabla_{\theta_1}\mathcal{L}$
end for

Bijective encoders for categorical data Many fairness datasets consist of categorical data, and often even continuous data is discretized before training. In this case, we will show that the optimal bijective representation can be easily computed. Consider the case of discrete samples $\boldsymbol{x}$ coming from a probability distribution $p(\boldsymbol{x})$ where each component x_i takes a value from a finite set $\{1, 2, \ldots, d_i\}$. Similar to the continuous case, our goal is to find bijections f_0 and f_1 that minimize the statistical distance of the latent distributions. Intuitively, we want to pair together inputs which have similar probabilities in both p_0 and p_1. In Lemma 5.4 we show that the solution which minimizes the statistical distance is obtained by sorting the inputs according to their probabilities in p_0 and p_1, and then matching inputs at the corresponding indices in these two sorted arrays. As this can result in a bad classification accuracy when inputs with different target labels get matched together, we can

obtain another representation by splitting inputs in two groups according to the predicted classification label and then matching inputs in each group using Lemma 5.4. We can trade off accuracy and fairness by randomly selecting one of the two mappings based on parameter γ.

Lemma 5.4. *Let $\mathcal{X} = \{\boldsymbol{x}_1, ..., \boldsymbol{x}_m\}$ and bijections $f_0, f_1 : \mathcal{X} \to \mathcal{X}$. Denote $i_1, i_2, ..., i_m$ and $j_1, ..., j_m$ permutations of $\{1, 2, ..., m\}$ such that $p_0(\boldsymbol{x}_{i_1}) \leq p_0(\boldsymbol{x}_{i_2}) \leq ... \leq p_0(\boldsymbol{x}_{i_m})$ and $p_1(\boldsymbol{x}_{j_1}) \leq p_1(\boldsymbol{x}_{j_2}) \leq ... \leq p_1(\boldsymbol{x}_{j_m})$. The encoders defined by mapping $f_0(\boldsymbol{x}_k) = \boldsymbol{x}_k$ and $f_1(\boldsymbol{x}_{j_k}) = \boldsymbol{x}_{i_k}$ are bijective representations with the smallest possible statistical distance.*

Statistical distance of true vs. estimated density In this work we assume access to a density of the inputs for both groups and we *provably guarantee* fairness with respect to *this* density. While it is sensible in the cases where the density estimate can be trusted (e.g., if it was provided by a regulatory agency), in many practical scenarios, and our experiments in Section 6, we only have an estimate $\hat{p}_0$ and $\hat{p}_1$ of the true densities p_0 and p_1. We now want to know how far off our guarantees are compared to the ones for the true density. The following theorem provides a way to theoretically bound the statistical distance between p_{Z_0} and p_{Z_1} using the statistical distance between $\hat{p}_{Z_0}$ and $\hat{p}_{Z_1}$.

Theorem 5.5. *Let $\hat{p}_0$ and $\hat{p}_1$ be density estimates such that $TV(\hat{p}_0, p_0) < \epsilon/2$ and $TV(\hat{p}_1, p_1) < \epsilon/2$, where TV stands for total variation between two distributions. If we denote latent distributions $f_0(\hat{p}_0)$ and $f_1(\hat{p}_1)$ as $\hat{p}_{Z_0}$ and $\hat{p}_{Z_1}$ then $\Delta(p_{Z_0}, p_{Z_1}) \leq \Delta(\hat{p}_{Z_0}, \hat{p}_{Z_1}) + \epsilon$.*

This theorem can be naturally combined with Lemma 5.2 to obtain a high probability upper bound on the statistical distance of the underlying true densities using estimated densities and a finite number of samples. Computing exact constants for the theorem is often not tractable, but as we will show experimentally, in practice bounds computed on the estimated distribution in fact bound adversarial accuracy on the true distribution. Moreover, for low-dimensional data relevant to fairness obtaining good estimates can be provably done for models such as Gaussian Mixture Models (Hardt & Price, 2015) and Kernel Density Estimation (Jiang, 2017). We can thus leverage the rich literature on density estimation (Rezende & Mohamed, 2015; Dinh et al., 2015; 2016; Kingma & Dhariwal, 2018; van den Oord et al., 2016a;c;b; Germain et al., 2015) to estimate $\hat{p}_0$ and $\hat{p}_1$. Importantly, FNF is agnostic to the concrete density estimation method (as we will show in Appendix C), and can thus benefit from future advances in the field. Finally, we note that density estimation has been successfully employed in a variety of security-critical areas such as fairness (Song et al., 2019), adversarial robustness (Wong & Kolter, 2020), and anomaly detection (Pidhorskyi et al., 2018).

6 Experimental Evaluation

In this section, we evaluate Fair Normalizing Flows (FNF) on several standard datasets from the fairness literature. We consider Adult and Crime from the UCI repository (Dua & Graff, 2017), Compas (Angwin et al., 2016), Law School (Wightman, 2017), and the Health Heritage Prize dataset. We preprocess Compas and Adult into categorical datasets by discretizing continuous features, and we keep the other datasets as continuous. Moreover, we preprocess the datasets by dropping uninformative features, facilitating the learning of a good density estimate, while keeping accuracy high (shown in Appendix B). We describe our full setup in detail in Appendix B. We will release all code, datasets, and preprocessing pipelines to ensure reproducibility of our results.

Evaluating Fair Normalizing Flows We first evaluate FNF's effectiveness in learning fair representations. For each dataset, we train different FNF models by varying the utility vs. fairness tradeoff parameter γ (see Algorithm 1). We estimate input densities using RealNVP (Dinh et al., 2016) for Health, MADE (Germain et al., 2015) for Adult and Compas, and Gaussian Mixture Models (GMMs) for the rest (we demonstrate that FNF is compatible with any differentiable prior by considering additional density estimation methods in Appendix C). For continuous datasets we use RealNVP as encoder architecture, while for categorical datasets we compute the optimal bijective representations using Lemma 5.4. Fig. 4 shows our results, each point representing a single model, with models on the right focusing on classification accuracy, and models on the left gradually increasing their fairness focus. The results in Fig. 4, averaged over 5 random seeds, indicate that FNF successfully reduces the statistical distance between representations of sensitive groups while maintaining high accuracy. We observe that for some datasets (e.g., Law School) enforcing fairness only slightly degrades accuracy, while for others there is a substantial drop (e.g., Crime). In such datasets where the label and sensitive

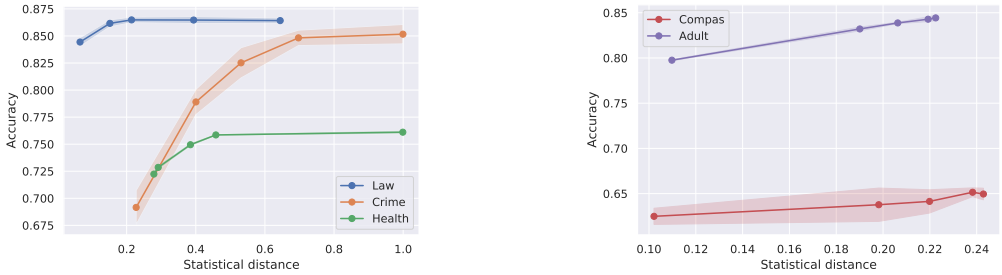

(a) Continuous datasets

(b) Categorical datasets

Figure 4: Fair Normalizing Flows (FNF) on continuous and categorical data. The points show different accuracy vs. statistical distance tradeoffs (with 95% confidence intervals from varied random seeds), demonstrating that FNF significantly reduces statistical distance while retaining high accuracy.

	Acc	Adv Acc $g \in \mathcal{G}$	Adv Acc $g \notin \mathcal{G}$	Max Adv Acc
ADV FORGETTING (Jaiswal et al., 2020)	85.99	66.68	74.50	✗
MAXENT-ARL (Roy & Boddeti, 2019)	85.90	50.00	85.18	✗
LAFTR (Madras et al., 2018)	**86.09**	72.05	84.58	✗
FNF (our work)	84.43	N/A	**59.56**	**61.12**

Table 1: Adversarial fair representation learning methods are only fair w.r.t. adversaries from a training family $\mathcal{G}$. while FNF provides a provable upper bound on the maximum accuracy of *any* adversary.

attribute are highly correlated we cannot achieve fairness and high accuracy simultaneously (Menon & Williamson, 2018; Zhao & Gordon, 2019). Overall, we see that FNF is generally insensitive to the random seed and can reliably enforce fairness. Recall that we have focused on minimizing statistical distance of learned representations because, as mentioned earlier, Madras et al. (2018) have shown that fairness metrics such as demographic parity, equalized odds and equal opportunity can all be bounded by statistical distance. For example, for Health FNF reduces the demographic parity distance of a classifier from 0.39 to 0.08 with an accuracy drop of 3.9% (we provide similar results showing FNF's good performance for equalized odds and equality of opportunity in Appendix C).

Bounding adversarial accuracy Recall that the guarantees provided by FNF hold for estimated densities $\hat{p}_0$ and $\hat{p}_1$. Namely, the maximum adversarial accuracy for predicting whether the latent representation $\boldsymbol{z}$ originates from distribution $\hat{\mathcal{Z}}_0$ or $\hat{\mathcal{Z}}_1$ is bounded by $(1 + \Delta(\hat{p}_{Z_0}, \hat{p}_{Z_1}))/2$. In this experiment, we investigate how well these guarantees transfer to the underlying distributions $\mathcal{Z}_0$ and $\mathcal{Z}_1$. In Fig. 5 we show our upper bound on the adversarial accuracy computed from the statistical distance using the estimated densities (diagonal dashed line), together with adversarial accuracies obtained by training an adversary, a multilayer perceptron (MLP) with two hidden layers of 50 neurons, for each model from Fig. 4. We also show 95% confidence intervals obtained using the Hoeffding bound from Lemma 5.2. We observe that our upper bound from the estimated densities $\hat{p}_0$ and $\hat{p}_1$ provides a tight upper bound on the adversarial accuracy for the true distributions $\mathcal{Z}_0$ and $\mathcal{Z}_1$. This demonstrates that, even though exact constants from Theorem 5.5 are intractable, our density estimate is good enough in practice, and our bounds hold for adversaries on the true distribution.

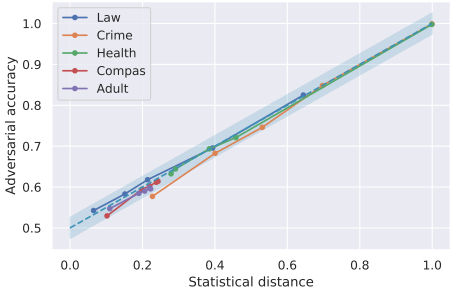

Figure 5: Bounding adversarial accuracy via FNF.

Comparison with adversarial training We now compare FNF with adversarial fair representation learning methods on Adult dataset: LAFTR-DP ($\gamma = 2$) (Madras et al., 2018), MaxEnt-ARL

($\alpha = 10$) (Roy & Boddeti, 2019), and Adversarial Forgetting ($\rho = 0.001, \delta = 1, \lambda = 0.1$) (Jaiswal et al., 2020). Adversarial training operates on a family of adversaries $\mathcal{G}$ trying to predict the sensitive attribute from the latent representation. Here, the families $\mathcal{G}$ are MLPs with 1 hidden layer of 8 neurons for Madras et al. (2018), and 2 hidden layers with 64 neurons and 50 neurons for Roy & Boddeti (2019) and Jaiswal et al. (2020), respectively. In Table 1 we show that these methods generally succeed in preventing adversaries from $\mathcal{G}$ to predict the sensitive attributes. However, we can still attack these representations using either larger MLPs (3 layers of 200 neurons for Madras et al. (2018)) or simple preprocessing steps (for Roy & Boddeti (2019); Jaiswal et al. (2020)) as proposed by Gupta et al. (2021) (essentially reproducing their results). Our results confirm findings from prior work (Feng et al., 2019; Elazar & Goldberg, 2018; Xu et al., 2020; Gupta et al., 2021): adversarial training provides no guarantees against adversaries outside $\mathcal{G}$. In contrast, FNF computes a provable upper bound on the accuracy of *any* adversary (i.e., $\mathcal{G} = \emptyset$) for the estimated input distribution, and Table 1 shows that this extends to the true distribution (as before). FNF thus learns representations with significantly lower adversarial accuracy with only minor decrease in task accuracy.

Algorithmic recourse with FNF We next experiment with using FNF's bijectivity to perform recourse, i.e., reverse an unfavorable outcome, which is considered to be fundamental to transparent and explainable algorithmic decision-making (Venkatasubramanian & Alfano, 2020; Sharma et al., 2020). To that end, we apply FNF with $\gamma = 1$ to the Law School dataset which has three features (after preprocessing): LSAT score, undergraduate GPA, and the college to which the student applied (ordered decreasingly in admission rate). For all rejected applicants, i.e., $\boldsymbol{x}$ such that $h(f_a(\boldsymbol{x})) = h(\boldsymbol{z}) = 0$, we compute the closest $\tilde{\boldsymbol{z}}$ (corresponding to a point $\tilde{\boldsymbol{x}}$ from the dataset) w.r.t. the ℓ_2-distance in latent space such that $h(\tilde{\boldsymbol{z}}) = 1$. We then linearly interpolate between $\boldsymbol{z}$ and $\tilde{\boldsymbol{z}}$ to find a (potentially crude) approximation of the closest point to $\boldsymbol{z}$ in latent space with positive prediction. Using the bijectivity of our encoders, we can compute the corresponding average feature change in the original space which would have caused a positive decision: increasing LSAT by 4.2 (non-whites) and 7.7 (whites), and increasing GPA by 0.7 (non-whites) and 0.6 (whites), where we only report recourse in the cases where the college does not change since this may not be actionable advice for certain applicants (Zhang et al., 2018; Ustun et al., 2019; Poyiadzi et al., 2020; Karimi et al., 2021). In Appendix C, we also show that, unlike prior work, FNF enables practical interpretability analyses.

Flow architectures In the next experiment we compare RealNVP encoder with the alternative encoder based on Neural Spline Flows architecture (Durkan et al., 2019), on the Crime dataset. In Table 2 we show the statistical distance and accuracy for models obtained using different values for the tradeoff parameter γ. We can observe that both flows offer similar performance. Note that FNF will only benefit from future advances in normalizing flows research, as it is orthogonal to the concrete flow architecture that is used for training.

	RealNVP		NSF	
γ	Δ	Acc	Δ	Acc
0.00	1.00	0.85	1.00	0.84
0.02	0.70	0.85	0.71	0.85
0.10	0.53	0.83	0.54	0.83
0.90	0.23	0.69	0.24	0.69

Table 2: Comparing flow architectures.

Transfer learning Unlike prior work, transfer learning with FNF requires no additional reconstruction loss since both encoders are invertible and thus preserve all information about the input data. To demonstrate this, we follow the setup from Madras et al. (2018) and train a model to predict the Charlson Index for the Health Heritage Prize dataset. We then transfer the learned encoder and train a classifier for the task of predicting the primary condition group. Our encoder reduces the statistical distance from 0.99 to 0.31 (this is independent of the label). For the primary condition group MSC2a3 we retain the accuracy at 73.8%, while for METAB3 it slightly decreases from 75.4% to 73.1%.

7 Conclusion

We introduced Fair Normalizing Flows (FNF), a new method for learning representations which ensure that no adversary can predict sensitive attributes. This guarantee is stronger than prior work which only considers adversaries from a restricted model family. The key idea is to use an encoder based on normalizing flows which allows computing the exact likelihood in the latent space, given an estimate of the input density. Our experimental evaluation on several datasets showed that FNF is flexible and can effectively enforce fairness without significantly sacrificing utility, while simultaneously allowing interpreting the learned representations and transferring to unseen tasks.

ETHICS STATEMENT

Since machine learning models have been shown to reinforce the human biases that are embedded in the training data, regulators and scientists alike are striving to propose novel regulations and algorithms to ensure the fairness of such models. Our method enables data producers to learn fair data representations that are guaranteed to be non-discriminatory regardless of the concrete downstream usecase. Since our method relies on accurate density estimates, we envision that the data regulators, whose tasks already include determining fairness criteria, data sources, and auditing results, would create a regulatory framework for density estimation that can then be realized by, e.g., industrial partners. Importantly, this would not require regulators to estimate the densities themselves. Nevertheless, data regulators would need to take great care when formulating such legislation since the potential negative effects of poor density estimates are still largely unexplored, both in the context of our work and in the broader field (particularly for high-dimensional data). In this setting, any data producer using our method would then be able to guarantee the fairness of all potential downstream consumer models.

REFERENCES

Aws Albarghouthi, Loris D'Antoni, Samuel Drews, and Aditya V. Nori. Fairsquare: probabilistic verification of program fairness. *Proc. ACM Program. Lang.*, 2017.

Julia Angwin, Jeff Larson, Surya Mattu, and Lauren Kirchner. Machine bias, 2016.

Solon Barocas and Andrew D. Selbst. Big data's disparate impact. *California Law Review*, 2016.

Osbert Bastani, Xin Zhang, and Armando Solar-Lezama. Probabilistic verification of fairness properties via concentration. *Proc. ACM Program. Lang.*, 2019.

Hugo Berard, Gauthier Gidel, Amjad Almahairi, Pascal Vincent, and Simon Lacoste-Julien. A closer look at the optimization landscapes of generative adversarial networks. 2020.

Tim Brennan, William Dieterich, and Beate Ehret. Evaluating the predictive validity of the compas risk and needs assessment system. *Criminal Justice and Behavior*, 2009.

Elliot Creager, David Madras, Jörn-Henrik Jacobsen, Marissa A. Weis, Kevin Swersky, Toniann Pitassi, and Richard S. Zemel. Flexibly fair representation learning by disentanglement. In *Proceedings of the 36th International Conference on Machine Learning*, 2019.

Laurent Dinh, David Krueger, and Yoshua Bengio. NICE: non-linear independent components estimation. In *3rd International Conference on Learning Representations*, 2015.

Laurent Dinh, Jascha Sohl-Dickstein, and Samy Bengio. Density estimation using real NVP. *CoRR*, 2016.

Dheeru Dua and Casey Graff. UCI machine learning repository, 2017.

Conor Durkan, Artur Bekasov, Iain Murray, and George Papamakarios. Neural spline flows. *Advances in Neural Information Processing Systems*, 2019.

Cynthia Dwork, Frank McSherry, Kobbi Nissim, and Adam D. Smith. Calibrating noise to sensitivity in private data analysis. In *Third Theory of Cryptography Conference*, 2006.

Cynthia Dwork, Moritz Hardt, Toniann Pitassi, Omer Reingold, and Richard S. Zemel. Fairness through awareness. In *Innovations in Theoretical Computer Science 2012*, 2012.

Harrison Edwards and Amos J. Storkey. Censoring representations with an adversary. In *4th International Conference on Learning Representations*, 2016.

Yanai Elazar and Yoav Goldberg. Adversarial removal of demographic attributes from text data. In *Proceedings of the 2018 Conference on Empirical Methods in Natural Language Processing*, 2018.

EU. Proposal for a regulation laying down harmonised rules on artificial intelligence, 2021.

Rui Feng, Yang Yang, Yuehan Lyu, Chenhao Tan, Yizhou Sun, and Chunping Wang. Learning fair representations via an adversarial framework. *CoRR*, abs/1904.13341, 2019.

Flaticon.com. Image, 2021.

FTC. Aiming for truth, fairness, and equity in your company's use of ai, 2021. URL https://www.ftc.gov/news-events/blogs/business-blog/2021/04/aiming-truth-fairness-equity-your-companys-use-ai.

Mathieu Germain, Karol Gregor, Iain Murray, and Hugo Larochelle. MADE: masked autoencoder for distribution estimation. In *Proceedings of the 32nd International Conference on Machine Learning*, 2015.

Ian J. Goodfellow, Jean Pouget-Abadie, Mehdi Mirza, Bing Xu, David Warde-Farley, Sherjil Ozair, Aaron C. Courville, and Yoshua Bengio. Generative adversarial nets. In *Advances in Neural Information Processing Systems 27*, 2014.

Arthur Gretton, Karsten M. Borgwardt, Malte J. Rasch, Bernhard Schölkopf, and Alexander J. Smola. A kernel method for the two-sample-problem. In *Advances in Neural Information Processing Systems 19*, 2006.

Aditya Grover, Christopher Chute, Rui Shu, Zhangjie Cao, and Stefano Ermon. Alignflow: Cycle consistent learning from multiple domains via normalizing flows. In *AAAI*, pp. 4028–4035. AAAI Press, 2020.

Umang Gupta, Aaron Ferber, Bistra Dilkina, and Greg Ver Steeg. Controllable guarantees for fair outcomes via contrastive information estimation. *CoRR*, abs/2101.04108, 2021.

Moritz Hardt and Eric Price. Tight bounds for learning a mixture of two gaussians. In Rocco A. Servedio and Ronitt Rubinfeld (eds.), *Proceedings of the Forty-Seventh Annual ACM on Symposium on Theory of Computing*, 2015.

Moritz Hardt, Eric Price, and Nati Srebro. Equality of opportunity in supervised learning. In *Advances in Neural Information Processing Systems 29*, 2016.

Yuzi He, Keith Burghardt, and Kristina Lerman. Learning fair and interpretable representations via linear orthogonalization. *CoRR*, abs/1910.12854, 2019.

Emiel Hoogeboom, Jorn W. T. Peters, Rianne van den Berg, and Max Welling. Integer discrete flows and lossless compression. In *NeurIPS*, pp. 12134–12144, 2019.

Matthew Jagielski, Michael J. Kearns, Jieming Mao, Alina Oprea, Aaron Roth, Saeed Sharifi-Malvajerdi, and Jonathan R. Ullman. Differentially private fair learning. In *Proceedings of the 36th International Conference on Machine Learning*, 2019.

Ayush Jaiswal, Daniel Moyer, Greg Ver Steeg, Wael AbdAlmageed, and Premkumar Natarajan. Invariant representations through adversarial forgetting. In *The Thirty-Fourth AAAI Conference on Artificial Intelligence*, 2020.

Heinrich Jiang. Uniform convergence rates for kernel density estimation. In Doina Precup and Yee Whye Teh (eds.), *Proceedings of the 34th International Conference on Machine Learning*, 2017.

Philips George John, Deepak Vijaykeerthy, and Diptikalyan Saha. Verifying individual fairness in machine learning models. In *Proceedings of the Thirty-Sixth Conference on Uncertainty in Artificial Intelligence*, 2020.

Kaggle. Health heritage prize. URL https://www.kaggle.com/c/hhp.

Toshihiro Kamishima, Shotaro Akaho, and Jun Sakuma. Fairness-aware learning through regularization approach. In *Data Mining Workshops (ICDMW)*, 2011.

Amir-Hossein Karimi, Bernhard Schölkopf, and Isabel Valera. Algorithmic recourse: from counterfactual explanations to interventions. In *ACM Conference on Fairness, Accountability, and Transparency*, 2021.

Thomas Kehrenberg, Myles Bartlett, Oliver Thomas, and Novi Quadrianto. Null-sampling for interpretable and fair representations. In *Computer Vision - ECCV 2020 - 16th European Conference*, 2020.

Amir E Khandani, Adlar J Kim, and Andrew W Lo. Consumer credit-risk models via machine-learning algorithms. *Journal of Banking & Finance*, 2010.

Diederik P. Kingma and Jimmy Ba. Adam: A method for stochastic optimization. In *3rd International Conference on Learning Representations*, 2015.

Diederik P. Kingma and Prafulla Dhariwal. Glow: Generative flow with invertible 1x1 convolutions. In *Advances in Neural Information Processing Systems 31*, 2018.

Diederik P. Kingma and Max Welling. Auto-encoding variational bayes. In *2nd International Conference on Learning Representations*, 2014.

Jiachun Liao, Chong Huang, Peter Kairouz, and Lalitha Sankar. Learning generative adversarial representations (GAP) under fairness and censoring constraints. *CoRR*, abs/1910.00411, 2019.

Xi Lin, Hui-Ling Zhen, Zhenhua Li, Qingfu Zhang, and Sam Kwong. Pareto multi-task learning. In *Advances in Neural Information Processing Systems 32*, 2019.

Stuart P. Lloyd. Least squares quantization in PCM. *IEEE Trans. Inf. Theory*, 1982.

Francesco Locatello, Gabriele Abbati, Thomas Rainforth, Stefan Bauer, Bernhard Schölkopf, and Olivier Bachem. On the fairness of disentangled representations. In *Advances in Neural Information Processing Systems 32*, 2019.

Christos Louizos, Kevin Swersky, Yujia Li, Max Welling, and Richard S. Zemel. The variational fair autoencoder. In *4th International Conference on Learning Representations*, 2016.

James MacQueen. Some methods for classification and analysis of multivariate observations. In *Proceedings of the fifth Berkeley symposium on mathematical statistics and probability*, 1967.

David Madras, Elliot Creager, Toniann Pitassi, and Richard S. Zemel. Learning adversarially fair and transferable representations. In *Proceedings of the 35th International Conference on Machine Learning*, 2018.

Natalia Martínez, Martín Bertrán, and Guillermo Sapiro. Minimax pareto fairness: A multi objective perspective. In *Proceedings of the 37th International Conference on Machine Learning*, 2020.

Daniel McNamara, Cheng Soon Ong, and Robert C. Williamson. Costs and benefits of fair representation learning. In *Proceedings of the 2019 AAAI/ACM Conference on AI, Ethics, and Society*, 2019.

Aditya Krishna Menon and Robert C. Williamson. The cost of fairness in binary classification. In *Conference on Fairness, Accountability and Transparency*, 2018.

Daniel Moyer, Shuyang Gao, Rob Brekelmans, Aram Galstyan, and Greg Ver Steeg. Invariant representations without adversarial training. In *Advances in Neural Information Processing Systems 31*, 2018.

Adam Paszke, Sam Gross, Francisco Massa, Adam Lerer, James Bradbury, Gregory Chanan, Trevor Killeen, Zeming Lin, Natalia Gimelshein, Luca Antiga, Alban Desmaison, Andreas Köpf, Edward Yang, Zachary DeVito, Martin Raison, Alykhan Tejani, Sasank Chilamkurthy, Benoit Steiner, Lu Fang, Junjie Bai, and Soumith Chintala. Pytorch: An imperative style, high-performance deep learning library. In *Advances in Neural Information Processing Systems 32*, 2019.

Stanislav Pidhorskyi, Ranya Almohsen, and Gianfranco Doretto. Generative probabilistic novelty detection with adversarial autoencoders. In *Advances in Neural Information Processing Systems 31*, 2018.

Rafael Poyiadzi, Kacper Sokol, Raúl Santos-Rodríguez, Tijl De Bie, and Peter A. Flach. FACE: feasible and actionable counterfactual explanations. In *AAAI/ACM Conference on AI, Ethics, and Society*, 2020.

Danilo Jimenez Rezende and Shakir Mohamed. Variational inference with normalizing flows. In *Proceedings of the 32nd International Conference on Machine Learning*, 2015.

Proteek Chandan Roy and Vishnu Naresh Boddeti. Mitigating information leakage in image representations: A maximum entropy approach. In *IEEE Conference on Computer Vision and Pattern Recognition*, 2019.

Anian Ruoss, Mislav Balunovic, Marc Fischer, and Martin T. Vechev. Learning certified individually fair representations. In *Advances in Neural Information Processing Systems 33*, 2020.

Shahar Segal, Yossi Adi, Benny Pinkas, Carsten Baum, Chaya Ganesh, and Joseph Keshet. Fairness in the eyes of the data: Certifying machine-learning models. *CoRR*, abs/2009.01534, 2020.

Shubham Sharma, Jette Henderson, and Joydeep Ghosh. CERTIFAI: A common framework to provide explanations and analyse the fairness and robustness of black-box models. In *AAAI/ACM Conference on AI, Ethics, and Society*, 2020.

Congzheng Song and Vitaly Shmatikov. Overlearning reveals sensitive attributes. In *8th International Conference on Learning Representations*, 2020.

Jiaming Song, Pratyusha Kalluri, Aditya Grover, Shengjia Zhao, and Stefano Ermon. Learning controllable fair representations. In *The 22nd International Conference on Artificial Intelligence and Statistics*, 2019.

Dustin Tran, Keyon Vafa, Kumar Krishna Agrawal, Laurent Dinh, and Ben Poole. Discrete flows: Invertible generative models of discrete data. In *NeurIPS*, pp. 14692–14701, 2019.

Caterina Urban, Maria Christakis, Valentin Wüstholz, and Fuyuan Zhang. Perfectly parallel fairness certification of neural networks. *Proc. ACM Program. Lang.*, 2020.

Ben Usman, Avneesh Sud, Nick Dufour, and Kate Saenko. Log-likelihood ratio minimizing flows: Towards robust and quantifiable neural distribution alignment. In *NeurIPS*, 2020.

Berk Ustun, Alexander Spangher, and Yang Liu. Actionable recourse in linear classification. In *Proceedings of the Conference on Fairness, Accountability, and Transparency*, 2019.

Aäron van den Oord, Sander Dieleman, Heiga Zen, Karen Simonyan, Oriol Vinyals, Alex Graves, Nal Kalchbrenner, Andrew W. Senior, and Koray Kavukcuoglu. Wavenet: A generative model for raw audio. In *The 9th ISCA Speech Synthesis Workshop*, 2016a.

Aäron van den Oord, Nal Kalchbrenner, Lasse Espeholt, Koray Kavukcuoglu, Oriol Vinyals, and Alex Graves. Conditional image generation with pixelcnn decoders. In *Advances in Neural Information Processing Systems 29*, 2016b.

Aäron van den Oord, Nal Kalchbrenner, and Koray Kavukcuoglu. Pixel recurrent neural networks. In *Proceedings of the 33nd International Conference on Machine Learning*, 2016c.

Laurens van der Maaten and Geoffrey Hinton. Visualizing data using t-sne. *Journal of Machine Learning Research*, 2008.

Suresh Venkatasubramanian and Mark Alfano. The philosophical basis of algorithmic recourse. In *Conference on Fairness, Accountability, and Transparency*, 2020.

Tianhao Wang, Zana Buçinca, and Zilin Ma. Learning interpretable fair representations. 2021.

Susan Wei and Marc Niethammer. The fairness-accuracy pareto front. *CoRR*, 2020.

Meredith Whittaker, Kate Crawford, Roel Dobbe, Genevieve Fried, Elizabeth Kaziunas, Varoon Mathur, Sarah Mysers West, Rashida Richardson, Jason Schultz, and Oscar Schwartz. *AI now report 2018*. AI Now Institute at New York University New York, 2018.

F. Linda Wightman. LSAC national longitudinal bar passage study, 2017.

Eric Wong and J. Zico Kolter. Learning perturbation sets for robust machine learning. *CoRR*, abs/2007.08450, 2020.

Qizhe Xie, Zihang Dai, Yulun Du, Eduard H. Hovy, and Graham Neubig. Controllable invariance through adversarial feature learning. In *Advances in Neural Information Processing Systems 30*, 2017.

Yilun Xu, Shengjia Zhao, Jiaming Song, Russell Stewart, and Stefano Ermon. A theory of usable information under computational constraints. In *8th International Conference on Learning Representations*, 2020.

Muhammad Bilal Zafar, Isabel Valera, Manuel Gomez-Rodriguez, and Krishna P. Gummadi. Fairness constraints: Mechanisms for fair classification. In *Proceedings of the 20th International Conference on Artificial Intelligence and Statistics*, 2017.

Richard S. Zemel, Yu Wu, Kevin Swersky, Toniann Pitassi, and Cynthia Dwork. Learning fair representations. In *Proceedings of the 30th International Conference on Machine Learning*, 2013.

Xin Zhang, Armando Solar-Lezama, and Rishabh Singh. Interpreting neural network judgments via minimal, stable, and symbolic corrections. In *Advances in Neural Information Processing Systems 31*, 2018.

Han Zhao and Geoffrey J. Gordon. Inherent tradeoffs in learning fair representations. 2019.

A APPENDIX

A.1 PROOFS

Here we present proofs of the theorems used in the paper.

Proof of Lemma 5.1 (Optimal adversary)

Proof. Here we prove Lemma 5.1 which states the form of an adversary $\mu\colon \mathbb{R}^d \to \{0,1\}$ that can achieve highest discrimination between $\mathcal{Z}_0$ and $\mathcal{Z}_1$. We start by rewriting the equation for statistical distance $\Delta(p_{Z_0}, p_{Z_1})$ as follows:

$$\Delta(p_{Z_0}, p_{Z_1}) = \sup_{\mu} \left|\mathbb{E}_{\boldsymbol{z}\sim\mathcal{Z}_0}[\mu(\boldsymbol{z})] - \mathbb{E}_{\boldsymbol{z}\sim\mathcal{Z}_1}[\mu(\boldsymbol{z})]\right| = \sup_{\mu} \left|\int_{\boldsymbol{z}} (p_{Z_0}(\boldsymbol{z}) - p_{Z_1}(\boldsymbol{z}))\mu(\boldsymbol{z})\, dz\right|. \quad (5)$$

To maximize the absolute value of the integral, we either have to maximize or minimize the integral $\int_{\boldsymbol{z}} (p_{Z_0}(\boldsymbol{z}) - p_{Z_1}(\boldsymbol{z}))\mu(\boldsymbol{z})\, dz$. Clearly, to maximize the integral we should choose function $\mu = \mathbb{1}_{\{p_{Z_0}(\boldsymbol{z}) \geq p_{Z_1}(\boldsymbol{z})\}}$, for which $\mu(\boldsymbol{z}) = 1$ if and only if $p_{Z_0}(\boldsymbol{z}) \geq p_{Z_1}(\boldsymbol{z})$, and 0 otherwise. Similarly, to minimize the integral we should choose function $\mu = \mathbb{1}_{\{p_{Z_0}(\boldsymbol{z}) \leq p_{Z_1}(\boldsymbol{z})\}}$ for which $\mu(\boldsymbol{z}) = 1$ if and only if $p_{Z_0}(\boldsymbol{z}) \leq p_{Z_1}(\boldsymbol{z})$, and 0 otherwise. In fact, it can be easily observed that both options result in the same absolute value of the integral so we can, without loss of generality, choose the first option $\mu^*(\boldsymbol{z}) = \mathbb{1}_{\{p_{Z_0}(\boldsymbol{z}) \leq p_{Z_1}(\boldsymbol{z})\}}$. This subsequently yields $\Delta(p_{Z_0}, p_{Z_1}) = \left|\mathbb{E}_{\boldsymbol{z}\sim\mathcal{Z}_0}[\mu^*(\boldsymbol{z})] - \mathbb{E}_{\boldsymbol{z}\sim\mathcal{Z}_1}[\mu^*(\boldsymbol{z})]\right|$. Moreover, we can also write $\Delta(p_{Z_0}, p_{Z_1}) = \left|\int_{\boldsymbol{z}} (p_{Z_1}(\boldsymbol{z}) - p_{Z_0}(\boldsymbol{z}))\mu^*(\boldsymbol{z})\, dz\right| = \left|\int_{\boldsymbol{z}} \max(0, p_{Z_1}(\boldsymbol{z}) - p_{Z_0}(\boldsymbol{z}))\, dz\right|$ (this will be used to prove Theorem 5.5). □

Proof of Lemma 5.2 (Finite sample estimate)

Proof. We start by plugging in the optimal adversary μ^* from Lemma 5.1 into the definition of statistical distance. Let μ^* be the optimal adversary defined in Lemma 5.1, namely $\mu^*(\boldsymbol{z}) = 1$ if and only if $p_{Z_0}(\boldsymbol{z}) < p_{Z_1}(\boldsymbol{z})$. We first write statistical distance in terms of the optimal adversary μ^*, then bound statistical distance using triangle inequality and finally apply Hoeffding's inequality on individual terms:

$$\begin{aligned}
\Delta(\mathcal{Z}_0, \mathcal{Z}_1) &= \sup_{\mu} \left|\mathbb{E}_{\boldsymbol{z}\sim\mathcal{Z}_0}[\mu(\boldsymbol{z})] - \mathbb{E}_{\boldsymbol{z}\sim\mathcal{Z}_1}[\mu(\boldsymbol{z})]\right| \\
&= \left|\mathbb{E}_{\boldsymbol{z}\sim\mathcal{Z}_0}[\mu^*(\boldsymbol{z})] - \mathbb{E}_{\boldsymbol{z}\sim\mathcal{Z}_1}[\mu^*(\boldsymbol{z})]\right| \\
&= \left|\mathbb{E}_{\boldsymbol{z}\sim\mathcal{Z}_0}[\mu^*(\boldsymbol{z})] - \frac{1}{n}\sum_{i=1}^{n} \mu^*(\boldsymbol{z}_0^i) + \frac{1}{n}\sum_{i=1}^{n} \mu^*(\boldsymbol{z}_0^i) - \frac{1}{n}\sum_{i=1}^{n} \mu^*(\boldsymbol{z}_1^i) + \frac{1}{n}\sum_{i=1}^{n} \mu^*(\boldsymbol{z}_1^i) - \mathbb{E}_{\boldsymbol{z}\sim\mathcal{Z}_1}[\mu^*(\boldsymbol{z})]\right| \\
&\leq \left|\mathbb{E}_{\boldsymbol{z}\sim\mathcal{Z}_0}[\mu^*(\boldsymbol{z})] - \frac{1}{n}\sum_{i=1}^{n} \mu^*(\boldsymbol{z}_0^i)\right| + \hat{\Delta}(\mathcal{Z}_0, \mathcal{Z}_1) + \left|\frac{1}{n}\sum_{i=1}^{n} \mu^*(\boldsymbol{z}_1^i) - \mathbb{E}_{\boldsymbol{z}\sim\mathcal{Z}_1}[\mu^*(\boldsymbol{z})]\right| \\
&\leq \hat{\Delta}(\mathcal{Z}_0, \mathcal{Z}_1) + \epsilon
\end{aligned}$$

where Hoeffding's inequality guarantees that with probability at least $(1 - 2\exp(-n\epsilon^2/2))^2$ first and last summand are at most $\epsilon/2$. □

Proof of Lemma 5.3 (Bounding statistical distance with symmetrized KL)

Proof. We can bound statistical distance $\Delta(p_{Z_0}, p_{Z_1})$ by noticing that because μ is a binary classifier, we have that $|\mu(\boldsymbol{z})| \leq 1$:

$$\Delta(p_{Z_0}, p_{Z_1}) = \sup_{\mu} \left|\int_{\boldsymbol{z}} (p_{Z_0}(\boldsymbol{z}) - p_{Z_1}(\boldsymbol{z}))\mu(\boldsymbol{z})\, dz\right| \leq \int_{\boldsymbol{z}} |p_{Z_0}(\boldsymbol{z}) - p_{Z_1}(\boldsymbol{z})|\, dz = TV(p_{Z_0}, p_{Z_1}).$$

Pinsker's inequality guarantees that $TV(p_{Z_0}, p_{Z_1})^2 \leq \frac{1}{2}KL(p_{Z_0}, p_{Z_1})$. Given that $TV(p_{Z_0}, p_{Z_1}) = TV(p_{Z_1}, p_{Z_0})$ we also have that $TV(p_{Z_0}, p_{Z_1})^2 \leq \frac{1}{2}KL(p_{Z_1}, p_{Z_0})$. In order to bound statistical distance we can now use $2\Delta(p_{Z_0}, p_{Z_1})^2 \leq 2TV(p_{Z_0}, p_{Z_1})^2 \leq \frac{1}{2}KL(p_{Z_0}, p_{Z_1}) + \frac{1}{2}KL(p_{Z_1}, p_{Z_0})$ which corresponds to our objective with symmetrized KL divergence used in Algorithm 1. □

Proof of Lemma 5.4 (Encoding for discrete distributions)

Proof. Without loss of generality we can assume that $f_0(\boldsymbol{x}_k) = \boldsymbol{x}_k$. Assume that $f_1(\boldsymbol{x}) = \boldsymbol{y}$ and $f_1(\boldsymbol{x}') = \boldsymbol{y}'$ where $p_0(\boldsymbol{x}) < p_0(\boldsymbol{x}')$ and $p_1(\boldsymbol{y}) > p_1(\boldsymbol{y}')$. Let $d_1 = |p_0(\boldsymbol{x}) - p_1(\boldsymbol{y})| + |p_0(\boldsymbol{x}') - p_1(\boldsymbol{y}')|$ and $d_2 = |p_0(\boldsymbol{x}) - p_1(\boldsymbol{y}')| + |p_0(\boldsymbol{x}') - p_1(\boldsymbol{y})|$. In the case when $p_1(\boldsymbol{y}) \leq p_0(\boldsymbol{x})$ or $p_1(\boldsymbol{y}') \geq p_0(\boldsymbol{x})$ it is easy to show that $d_1 = d_2$. Now, in the case when $p_0(\boldsymbol{x}) < p_1(\boldsymbol{y}') < p_0(\boldsymbol{x}) < p_1(\boldsymbol{y})$, we can see that $d_2 \leq d_1 - (p_0(\boldsymbol{x}) - p_1(\boldsymbol{y}')) < d_1$. Similarly, when $p_0(\boldsymbol{x}) < p_1(\boldsymbol{y}') < p_1(\boldsymbol{y}) < p_0(\boldsymbol{x})$, we can see that $d_2 \leq d_1 - (p_1(\boldsymbol{y}) - p_1(\boldsymbol{y}')) < d_1$. In all cases, $d_2 \leq d_1$, which means that if we swap $f_1(\boldsymbol{x})$ and $f_1(\boldsymbol{x}')$ total variation either decreases or stays the same. We can repeatedly swap such pairs, and once there are no more swaps to do, we arrive at the condition of the lemma where two arrays are sorted the same way.

□

Proof of Theorem 5.5 (True and approximate distributions)

Proof. Let $a \in \{0, 1\}$ be a sensitive attribute, and assume that $TV(\hat{p}_a, p_a) < \epsilon/2$. Recall that change of variables for probability densities gives us that for the representation $\boldsymbol{z} = f_a(\boldsymbol{x})$ we have, similar as in Eq. (4), $p_{Z_a}(\boldsymbol{z}) = p_a(\boldsymbol{x}) \left|\det \frac{\partial f_a(\boldsymbol{x})}{\partial \boldsymbol{x}}\right|^{-1}$ and $\hat{p}_{Z_a}(\boldsymbol{z}) = \hat{p}_a(\boldsymbol{x}) \left|\det \frac{\partial f_a(\boldsymbol{x})}{\partial \boldsymbol{x}}\right|^{-1}$. Then, using those formulas together with the change of variables rule for multivariate integrals we derive:

$$
\begin{aligned}
TV(\hat{p}_{Z_a}, p_{Z_a}) &= \int_{\boldsymbol{z}} |\hat{p}_{Z_a}(\boldsymbol{z}) - p_{Z_a}(\boldsymbol{z})| \, dz \\
&= \int_{\boldsymbol{x}} |\hat{p}_{Z_a}(f_a(\boldsymbol{x})) - p_{Z_a}(f_a(\boldsymbol{x}))| \left|\det \frac{\partial f_a(\boldsymbol{x})}{\partial \boldsymbol{x}}\right| \, dx \\
&= \int_{\boldsymbol{x}} \left| \hat{p}_a(\boldsymbol{x}) \left|\det \frac{\partial f_a(\boldsymbol{x})}{\partial \boldsymbol{x}}\right|^{-1} - p_a(\boldsymbol{x}) \left|\det \frac{\partial f_a(\boldsymbol{x})}{\partial \boldsymbol{x}}\right|^{-1} \right| \left|\det \frac{\partial f_a(\boldsymbol{x})}{\partial \boldsymbol{x}}\right| \, dx \\
&= \int_{\boldsymbol{x}} |\hat{p}_a(\boldsymbol{x}) - p_a(\boldsymbol{x})| \, dx \\
&= TV(\hat{p}_a, p_a) \\
&< \epsilon/2.
\end{aligned}
$$

We will also use the observation from the proof of Lemma 5.1 which states that

$$
\Delta(p_{Z_0}, p_{Z_1}) = \left| \int_{\boldsymbol{z}} \max(0, p_{Z_1}(\boldsymbol{z}) - p_{Z_0}(\boldsymbol{z})) \, dz \right|.
$$

We can now observe that the following inequality holds:

$$
\max(0, p_{Z_0}(\boldsymbol{z}) - p_{Z_1}(\boldsymbol{z})) \leq |p_{Z_0}(\boldsymbol{z}) - \hat{p}_{Z_0}(\boldsymbol{z})| + \max(0, \hat{p}_{Z_0}(\boldsymbol{z}) - \hat{p}_{Z_1}(\boldsymbol{z})) + |\hat{p}_{Z_1}(\boldsymbol{z}) - p_{Z_1}(\boldsymbol{z})|
$$

Integrating both sides yields:

$$
\begin{aligned}
\Delta(p_{Z_0}, p_{Z_1}) &\leq TV(p_{Z_0}(\boldsymbol{z}), \hat{p}_{Z_0}(\boldsymbol{z})) + \Delta(\hat{p}_{Z_0}, \hat{p}_{Z_1}) + TV(p_{Z_1}(\boldsymbol{z}), \hat{p}_{Z_1}(\boldsymbol{z})) \\
&\leq \Delta(\hat{p}_{Z_0}, \hat{p}_{Z_1}) + \epsilon
\end{aligned}
$$

Here last inequality follows from the previously proved inequality $TV(\hat{p}_{Z_a}, p_{Z_a}) < \epsilon/2$, applied for both $a = 0$ and $a = 1$. □

B Experimental Setup

In this section, we provide the full specification of our experimental setup. We first discuss the datasets considered and the corresponding preprocessing methods employed. We empirically validate that our preprocessing maintains high accuracy on the respective prediction tasks. Finally, we specify the hyperparameters and computing resources for the experiments in Section 6.

Table 3: Statistics for train, validation, and test datasets. In general, the label (y) and sensitive attribute (a) distributions are highly skewed, which is why we report balanced accuracy.

		SIZE	$a = 1$	$y = 1 \mid a = 0$	$y = 1 \mid a = 1$	$y = 1$
ADULT	TRAIN	24 129	32.6%	28.5%	21.6%	24.9%
	VALIDATION	6033	31.9%	28.3%	19.9%	24.9%
	TEST	15 060	32.6%	27.9%	19.1%	24.6%
COMPAS	TRAIN	3377	60.6%	60.9%	46.8%	52.3%
	VALIDATION	845	60.0%	60.1%	46.9%	52.2%
	TEST	1056	58.9%	61.8%	51.3%	55.6%
CRIME	TRAIN	1276	42.3%	71.3%	17.8%	48.7%
	VALIDATION	319	40.8%	78.8%	21.5%	55.5%
	TEST	399	43.1%	74.9%	16.3%	49.6%
HEALTH	TRAIN	139 785	35.7%	79.0%	48.3%	68.0%
	VALIDATION	34 947	35.6%	79.3%	49.2%	68.6%
	TEST	43 683	35.4%	78.8%	48.3%	68.0%
LAW	TRAIN	55 053	18.0%	28.5%	21.6%	27.3%
	VALIDATION	13 764	17.5%	28.3%	19.9%	26.8%
	TEST	17 205	17.5%	27.9%	19.1%	26.3%

B.1 DATASETS

We consider five commonly studied datasets from the fairness literature: Adult and Crime from the UCI machine learning repository (Dua & Graff, 2017), Compas (Brennan et al., 2009), Law School (Wightman, 2017), and the Health Heritage Prize (Kaggle) dataset. Below, we briefly introduce each of these datasets and discuss whether they contain personally identifiable information, if applicable. We preprocess Adult and Compas into categorical datasets by discretizing continuous features, keeping the other datasets as continuous. We drop rows and columns with missing values. For each dataset, we first split the data into training and test set, using the original splits wherever possible and a 80% / 20% split of the original dataset otherwise. We then further sample 20% of the training set to be used as validation set. Table 3 displays the dataset statistics for each of these splits. Finally, we drop uninformative features to facilitate density estimation. We show that the removal of these features does not significantly affect the predictive utility of the data in Table 4.

Adult

The Adult dataset, also known as Census Income dataset, was extracted from the 1994 Census database by Barry Becker and is provided by the UCI machine learning repository (Dua & Graff, 2017). It contains 14 attributes: age, workclass, fnlwgt, education, education-num, marital-status, occupation, relationship, race, sex, capital-gain, capital-loss, hours-per-week, and native-country. The prediction task is to determine whether a person makes over $50\,000$ US dollars per year. We consider sex as the protected attribute, and we discretize the dataset by keeping only the categorical columns relationship, workclass, marital-status, race, occupation, education-num, and education.

Compas

The Compas (Brennan et al., 2009) dataset was procured by ProPublica, and contains the criminal history, jail and prison time, demographics, and COMPAS risk scores for defendants from Broward County from 2012 and 2013. Through a public records request, ProPublica obtained two years worth of COMPAS scores ($18\,610$ people) from the Broward County Sheriff's Office in Florida. This data was then augmented with public criminal records from the Broward County Clerk's Office website.

Table 4: Classification accuracy before and after removing uninformative features during preprocessing. For each dataset we train a multi-layer perceptron (MLP) with the same architecture on the original and preprocessed data and report the average accuracy with standard deviation for five different random seeds. We can observe that the accuracy only decreases slightly after preprocessing.

	Accuracy (%)	
	Original	Preprocessed
Adult	85.0 ($\pm$ 0.001)	84.4 ($\pm$ 0.001)
Compas	65.3 ($\pm$ 0.003)	65.0 ($\pm$ 0.003)
Crime	85.5 ($\pm$ 0.003)	85.2 ($\pm$ 0.004)
Health	80.1 ($\pm$ 0.002)	76.1 ($\pm$ 0.001)
Law	88.2 ($\pm$ 0.006)	86.4 ($\pm$ 0.001)

Furthermore, jail records were obtained from the Browards County Sheriff's Office, and public incarceration records were downloaded from the Florida Department of Corrections website. The task consists of predicting recidivsm within two years for all individuals. We only consider Caucasian and African-American individuals and use race as the protected attribute. We discretize the continuous features age, diff-custody, diff-jail, and priors-count, and we remove all other features except for sex, c-charge-degree, and v-score-text.

Crime

The Communities and Crime dataset combines socio-economic data from the 1990 US Census, law enforcement data from the 1990 US LEMAS survey, and crime data from the 1995 FBI UCR. It was created by Michael Redmond and is provided by the UCI machine learning repository (Dua & Graff, 2017). The dataset contains 128 attributes such as county, population, per capita income, and number of immigrants. The task consists of predicting whether the number of violent crimes per population for a given community is above or below the median. We consider race as the protected attribute, which we set to 1 if the percentage of white people divided by 5 is smaller than the percentage of black, asian, and hispanic individuals, and to 0 otherwise. We keep the following 6 features: racePctWhite, pctWInvInc, PctFam2Par, PctKids2Par, PctYoungKids2Par, PctKidsBornNeverMar.

Health

The Health dataset was created for the Heritage Health Prize (Kaggle) competition on Kaggle and contains medical records of over $55\,000$ patients. We consider the merged claims, drug count, lab count, and members sheets, which have a total of 18 attributes. The identity of individual patients and health care providers, as well as other individual identifiable information, has been removed from the datasets to protect the privacy of those involved and to comply with applicable law. We consider age as the protected attribute, which we binarize to patients above and below 60 years. The task is to predict the maximum Charlson Comordbidity Index, which predicts 10-year survival in patients with multiple comorbities. We drop all but the following features: DrugCount-total, DrugCount-months, no-Claims, no-Providers, PayDelay-total, PrimaryConditionGroup, Specialty, ProcedureGroup, and PlaceSvc. For the transfer learning experiments we follow Madras et al. (2018) and omit the primary condition group labels from the set of features and try to predict them from the latent representation without explicitly optimizing for the task.

Law School

The Law School (Wightman, 2017) dataset contains admissions data from 25 law schools over the 2005, 2006, and in some cases 2007 admission cycles, providing information on over $100\,000$ individual applications. The data was procured by Project SEAPHE and was cleaned to adhere to high standards of data privacy. Concretely, when the school, race, year, and gender information for enrolled students produced cells of fewer than five subjects, the cells were combined to minimize reidentification risk. The attributes are law school, year of fall term, LSAT score, undergraduate GPA,

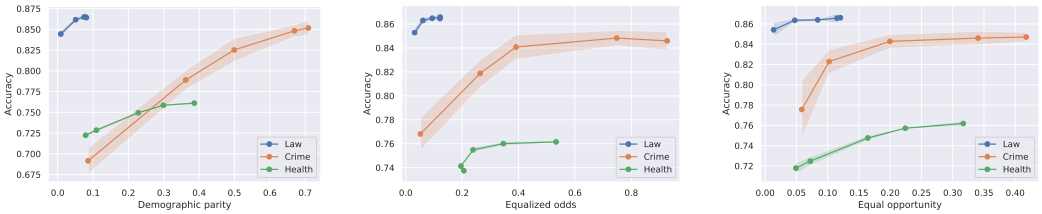

(a) Demographic parity (b) Equalized odds (c) Equal opportunity

Figure 6: Tradeoff between accuracy and various fairness metrics (demographic parity, equalized odds, equal opportunity) when using Fair Normalizing Flows (FNF).

race, gender, and in-state residency. We consider race as the protected attribute, which we binarize to white and non-white. We remove all features but the LSAT score, undergraduate GPA, and the college to which the student applied (ordered by decreasing admission rate).

B.2 Training details

Our code is implemented in PyTorch (Paszke et al., 2019).

Computing resources We run all experiments on a desktop PC using a single GeForce RTX 2080 Ti GPU and 16-core Intel(R) Core(TM) i9-9900K CPU @ 3.60GHz.

Hyperparameters for main experiments For Crime we estimate input density using Gaussian Mixture Model (GMM) with 4 components for $a = 0$ and 2 components for $a = 1$. For Law we use GMM with 8 components for both groups. Health dataset requires more complex density estimation so we use RealNVP (Dinh et al., 2016) with 4 blocks of 20 neurons each. For categorical datasets, Adult and Compas, we perform density estimation using MADE (Germain et al., 2015), which is represented using network of 2 hidden layers with 50 neurons.

We represent flow encoders using RealNVP with 4 blocks for Crime and Law, and 6 blocks for Health. Crime and Law use batch size 128, initial learning rate 0.01 and weight decay 0.0001, while Health uses batch size 256, initial learning rate 0.001 and weight decay 0. Training is performed using Adam (Kingma & Ba, 2015) optimizer. We use 60, 100, and 80 epochs for Crime, Law and Health, respectively. These parameters were chosen based on the performance on validation set.

For experiments in Fig. 4, we trained with the following 5 values for γ for respective datasets: 0, 0.02, 0.1, 0.2, 0.9 for Crime, 0, 0.001, 0.02, 0.1, 0.9 for Law, 0, 0.05, 0.1, 0.5, 0.95 for Health. Training for 1 epoch takes around 1 second for Crime, 5 seconds for Law, and 30 seconds for Health.

C Additional Experiments

In this section we present additional experimental results.

Compatibility with other fairness metrics In Section 6 we focused on presenting results on statistical distance, as it can bound various fairness metrics Madras et al. (2018). In constrast, here we provide more detailed experiments with three common group fairness metrics: demographic parity, equalized odds, and equality of opportunity. We demonstrate the tradeoff between these metrics and downstream accuracy in Fig. 6. We observe that FNF achieves high rates of demographic parity, equalized odds, and equality of opportunity with only small decreases in classification accuracy (similar to the results for the statistical distance showed in Fig. 4).

Compatibility with different scalarization schemes Since fairness and accuracy are often competing objectives, they merit a treatment from multi-objective optimization. Here, we investigate the scalarization scheme proposed by Wei & Niethammer (2020) and replace our objective $\gamma(\mathcal{L}_0 + \mathcal{L}_1) + (1 - \gamma)\mathcal{L}_{clf}$, obtained via convex scalarization,

with the Chebyshev scalarization scheme $\max\{\gamma(\mathcal{L}_0 + \mathcal{L}_1), (1-\gamma)\mathcal{L}_{clf}\}$, where we use the same normalization for $\mathcal{L}_0$, $\mathcal{L}_1$, and $\mathcal{L}_{clf}$ as Wei & Niethammer (2020). We evaluate the schemes for a large range of γ values on the Crime dataset and compute the Area Under the Curve (AUC) with the trapezoidal rule. The convex scalarization yields an AUC of 0.6036, whereas the Chebyshev scalarization attains an AUC of 0.6051. Moreover, we aggregate the results in Fig. 7. In general, we observe that the convex scalarization slightly outperforms the Chebyshev scalarization scheme. We believe that this is due to two reasons, (i) the Pareto curve is almost convex, which is why the convex scalarization performs well, and (ii) the stochasticity of gradient-based optimization. We consider more advanced multi-objective optimization methods Lin et al. (2019); Martínez et al. (2020) an interesting direction for future work.

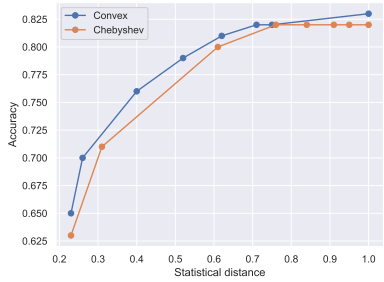

Figure 7: Different scalarization schemes.

Compatibility with different priors In the following experiment, we demonstrate that FNF is compatible with any differentiable estimate of p_0 and p_1. We consider Crime with the same setup as before, but with 3 different priors: a GMM with $k = 3$ components, an autoregressive prior, and a RealNVP flow (Dinh et al., 2016). For each of these priors, we train an encoder using FNF and a classifier on top of the learned representations. Fig. 8 shows the tradeoff between the statistical distance and accuracy for each of the priors. Based on these results, we can conclude that FNF achieves similar results for each of the priors, empirically demonstrating the flexibility of our approach.

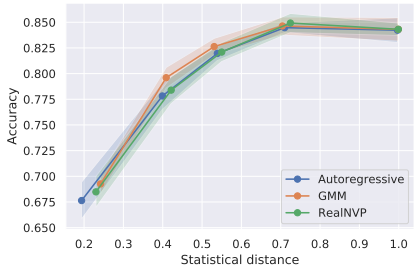

Figure 8: Different priors used with FNF.

Interpreting the representations We now show that the bijectivity of FNF enables interpretability analyses, an active area of research in fair representation learning (He et al., 2019; Kehrenberg et al., 2020; Wang et al., 2021). To that end, we consider the Crime dataset where for a community $\boldsymbol{x}$: (i) race (non-white vs. white majority) is the sensitive attribute a, (ii) the percentage of whites (highly correlated with, but not entirely predictive of the sensitive attribute) is in the feature set, and (iii) the label y strongly correlates with the sensitive attribute. We encode every community $\boldsymbol{x} \sim p_a$ as $\boldsymbol{z} = f_a(\boldsymbol{x})$ and compute the corresponding community with opposite sensitive attribute that is also mapped to $\boldsymbol{z}$, i.e., $\tilde{\boldsymbol{x}} = f^{-1}_{(1-a)}(\boldsymbol{z})$ (usually not in the dataset), yielding a matching between both distributions. We visualize the t-SNE (van der Maaten & Hinton, 2008) embeddings of this mapping for $\gamma \in \{0, 1\}$ in Fig. 9, where the dots are communities $\boldsymbol{x}$ and the crosses are the corresponding $\tilde{\boldsymbol{x}}$. We run k-means (MacQueen, 1967; Lloyd, 1982) on all points with $a = 1$ and show the matched clusters for points with $a = 0$ (e.g., red clusters are matched). For $\gamma = 0$, where FNF only minimizes the classification loss $\mathcal{L}_{clf}$, we observe a dichotomy between $\boldsymbol{x}$ and $\tilde{\boldsymbol{x}}$, since the encoder learns to match real points $\boldsymbol{x}$ with high likelihood to points $\tilde{\boldsymbol{x}}$ with low likelihood, yielding both high task utility (due to (iii)), but also high statistical distance (due to (ii)). For example, the red cluster has an average log-likelihood of -4.3 for $\boldsymbol{x}$ and -130.1 for $\tilde{\boldsymbol{x}}$. In contrast, for $\gamma = 1$ FNF minimizes only the KL-divergence losses $\mathcal{L}_0 + \mathcal{L}_1$, and thus learns to match points of roughly equal likelihood to the same latent point z such that the optimal adversary can no longer recover the sensitive attribute. Accordingly, the red cluster has an average log-likelihood of -2.8 for $\boldsymbol{x}$ and -3.0 for $\tilde{\boldsymbol{x}}$.

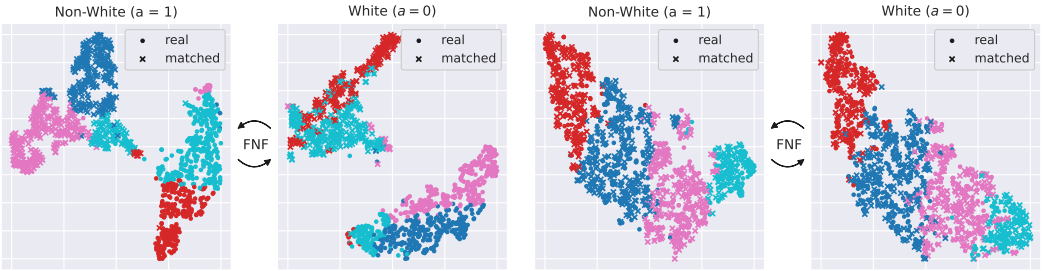

(a) $\gamma = 0$ (b) $\gamma = 1$

Figure 9: Visualizing k-means clusters on t-SNE embeddings of mappings between real points from the Crime dataset and their corresponding matches from the opposite attribute distribution.